15 July 1998

ELSEVIER

Optics Communications 153 (1998) 1–4

OPTICS COMMUNICATIONS

Real time 3D fluorescence microscopy by two beam interference illumination

M.A.A. Neil, R. Juškaitis, T. Wilson *

Department of Engineering Science, University of Oxford, Parks Road, Oxford OX1 3PJ, UK

Received 26 January 1998; revised 15 April 1998; accepted 20 April 1998

Abstract

We describe a method of obtaining optically sectioned fluorescence images in a widefield conventional microscope by interfering two beams on an object so as to illuminate it with a single spatial frequency fringe pattern. Images taken at three spatial positions of the fringe pattern are processed in real time to produce optically sectioned images which are substantially similar to those obtained with confocal microscopes.

1. Introduction

The widespread use of the confocal microscope in fields as diverse as semiconductor industry and the life sciences lies in its ability to produce high resolution images of three-dimensional volume structures. This is achievable because these instruments possess an optical sectioning property whereby only those object features which lie close to the plane of focus are imaged efficiently [1–3]. This permits a 'through focus' series of optical slices to be recorded and displayed in a variety of ways. The origin of the optical sectioning property in the confocal scanning microscope lies in the use of a pin-hole aperture placed in front of the photodetector which physically prevents light originating in out-of-focus planes reaching the detector and hence contributing to the image. This results in an optical system in which all spatial frequencies within the transfer function attenuate with defocus. This is true for both the brightfield and fluorescence imaging modes. For the conventional microscope, on the other hand, not all spatial frequencies attenuate with defocus and hence those instruments do not exhibit the optical sectioning or depth discrimination of confocal microscopes.

However, the conventional microscope does have some inherent advantages over the confocal in the sense that scanning is not necessary and the whole image is obtained in real time. Indeed, if we examine the transfer functions in detail for both the conventional brightfield and fluorescence case we find that it is *only* the zero spatial frequency which does *not* attenuate with defocus. This observation suggests the basis of a method to obtain optically sectioned images from a conventional wide-field microscope using a standard extended illumination source. In this approach the illumination system is modified so as to project a single spatial frequency grid pattern onto the object. The microscope will then image the grid pattern efficiently only on those portions of the object that are in focus. We can therefore obtain an optically sectioned image of the object by extracting only those parts of the image where the grid pattern is visible. The grid pattern itself then may be removed in a variety of ways the simplest of which, is to mathematically process three images obtained at three spatial positions of the grid. The system has previously been demonstrated in the brightfield mode and produced images that are substantially similar to those obtained with traditional confocal microscopes [4].

2. The principle

This principle of operation is equally applicable to the fluorescence case but an attractive alternative exists. In this

* Corresponding author. E-mail: tony.wilson@eng.ox.ac.uk

0030-4018/98/$19.00
PII S0030-4018(98)00210-7

case since, rather than project the image of a physical grid via a lens onto the object, it is possible to illuminate the specimen directly with the fringe pattern created by interfering two plane waves which are incident on the object at angles $\pm\theta$ to the optic axis. In this way a fringe pattern is formed of period $\lambda/(2\sin\theta)$, where λ is the wavelength. Fluorescent emission from the object that has been stimulated by this illuminating intensity pattern will possess the same spatial intensity modulation. If the fluorescent emission is then imaged with a conventional lens system then that image will be similarly modulated depending on the optical transfer function of the lens system. As the imaging is now incoherent, the fringes will only be significantly visible on the parts of the image that are in focus and the same mathematical processing as before can be performed to extract a sectioned image.

This approach has a number of attractions. The most significant is that no optical components other than mirrors and beamsplitters are required in the illumination path, which allows the approach to be used for fluorescence excitation at wavelengths where good quality optics are not readily available. Since the fringe pattern is uniform in depth along the optic axis, through the depth of the object, the alignment problems usually associated with confocal systems are virtually eliminated. In principle the system even allows multiple depth planes to be imaged simultaneously using separately focused cameras. The approach also has advantages in terms of aberrations. Firstly, because the illumination field contains a single spatial frequency, it is highly insensitive to aberrations. Furthermore, fringe distortions introduced by the specimen are of secondary importance as it is the relative phase shifts of the fringe pattern that matters for our algorithm. The effects of aberrations are thus only accumulated in a single pass through the fluorescence imaging system, and even here the need to use lenses corrected chromatically at both illuminating and detecting wavelengths is removed.

3. Analysis

The optical system, shown in Fig. 1, now simply consists of two laser beams which illuminate the object, characterised by a fluorescence function $f(t_1,w_1)$. The final image is recorded by a CCD in the image plane (t,w). The image intensity is given by

$$I(t,w) = \int\int S(t_1) f(t_1,w_1) \left| h(t_1+t, w_1+w) \right|^2 \mathrm{d}t_1\, \mathrm{d}w_1, \tag{1}$$

where $S(t_1)$ denotes the intensity of the fringe pattern caused by the interfering laser beams, h represents the point spread function of the imaging lens. We have also elected to work in optical co-ordinates [1,5] (t,w) which are related to real co-ordinates (x,y) through $(t,w) = (2\pi/\lambda)(x,y)n\sin\alpha$ where $n\sin\alpha$ is the numerical aperture and λ denotes the fluorescence wavelength.

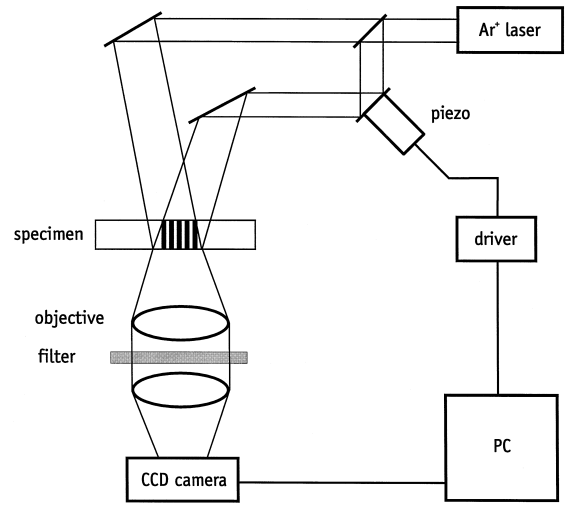

Fig. 1. Schematic diagram of the optical arrangement.

The illumination pattern $S(t_1)$ now takes the form

$$S(t_1) = 1 + m\cos(\nu t_1 + \phi_0), \tag{2}$$

where ν denotes the normalised spatial frequency which is related to actual fringe period Λ by $\nu = \lambda/(\Lambda n\sin\alpha)$, m denotes the modulation depth and ϕ_0 is an arbitrary spatial phase. If we substitute Eq. (2) into Eq. (1) we obtain

$$I(t,w) = I_0 + I_c\cos\phi_o - I_s\sin\phi_0, \tag{3}$$

where I_0 is given by $S(t_1) = 1$ in Eq. (1) and denotes, of course, a conventional fluorescence image. I_c and I_s, on the other hand, represent images corresponding to illumination by functions $S(t_1) = m\cos(\nu t_1)$ and $S(t_1) = m\sin(\nu t_1)$ respectively which are attenuated with defocus in the imaging stage. This suggests that as in the bright-field case, if we were to separate I_c and I_s from I_0 and form $I_p = (I_s^2 + I_c^2)^{1/2}$ we would achieve both an optically sectioned image and remove the fringe pattern. We can readily achieve this by taking three images I_1, I_2, I_3 at relative spatial phases corresponding to $\phi_0 = 0°$, 120° and 240° respectively. We can now obtain the optically sectioned image, which does not contain I_0, by calculating

$$I_p = \frac{\sqrt{2}}{3}\left\{(I_1-I_2)^2 + (I_1-I_3)^2 + (I_2-I_3)^2\right\}^{1/2}, \tag{4}$$

similarly the conventional image, I_0, may be recovered from

$$I_0 = \frac{I_1+I_2+I_3}{3}. \tag{5}$$

In this way both a conventional and optically sectioned image may be formed simultaneously from the same data.

It is usual to demonstrate and quantify the optical sectioning property of confocal instruments by measuring

the detected signal as a thin fluorescent sheet is scanned axially through focus. In order to calculate this response we set $f(t_1,w_1)=1$ in Eq. (1) and note that the processing of Eq. (4) is equivalent to setting $S(t_1)\sim\exp(j\nu t_1)$ and taking the modulus of the result. This gives the detected image signal as a function of defocus u

$$I_p(u)=\left|\int\int \exp(j\nu t_1)\left|h(u;t_1,w_1)\right|^2 \mathrm{d}t_1\,\mathrm{d}w_1\right|. \tag{6}$$

If we now introduce the pupil function $P(u;\xi,\eta)$ through the Fourier transform of the amplitude point spread function $h(u;t,w)$ we may write

$$I_p(u)=\left|\int\int P(u;\xi,\eta)P^*(u;\xi-\tilde{w},\eta)\,\mathrm{d}\xi\,\mathrm{d}n\right| =|g(u,\nu)|, \tag{7}$$

where $g(u,\nu)=P\otimes P^*$ where $\otimes$ represents the convolution operation and the asterisk denotes the complex conjugate.

We note that $g(u,\nu)$ is formally identical to the optical transfer function of a conventional fluorescence microscope. The function can be evaluated numerically but it will be more useful to use an approximation due to Stokseth [6], which permits us to write

$$g(u,\nu)=(1-0.69\nu+0.0076\nu^2+0.043\nu^4)\times\left\{2\frac{J_1[u\nu(1-\nu/2)]}{u\nu(1-\nu/2)}\right\}, \tag{9}$$

which confirms that optical sectioning is present in the same fashion as in confocal systems. The strength of the sectioning depends, of course, on the choice of ν and disappears when $\nu=0$ which is to be expected.

4. Experimental

Fig. 1 shows the experimental configuration used to produce optically sectioned fluorescence images in real time. 488 nm wavelength light from an Ar^+ laser split into two beams which were caused to interfere at the object so as to create the fringe pattern on the object. A 100× Leica Pl Apo 1.4 numerical aperture objective lens was used together with the corresponding Leica tube lens and appropriate filters passing wavelength longer than 580 nm. Images were captured with a CCD camera and transferred to a Matrox Meteor frame grabber. The fringe spatial

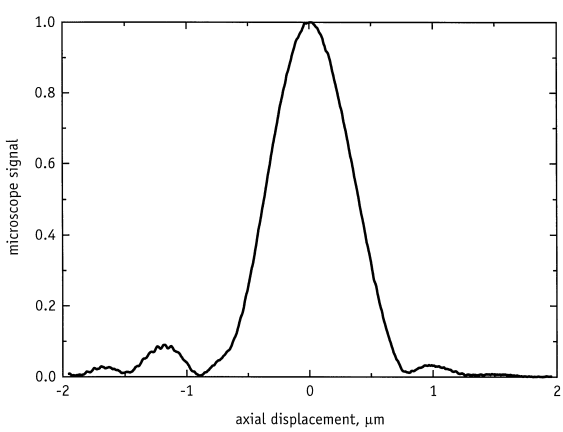

Fig. 2. The measured axial response of the system.

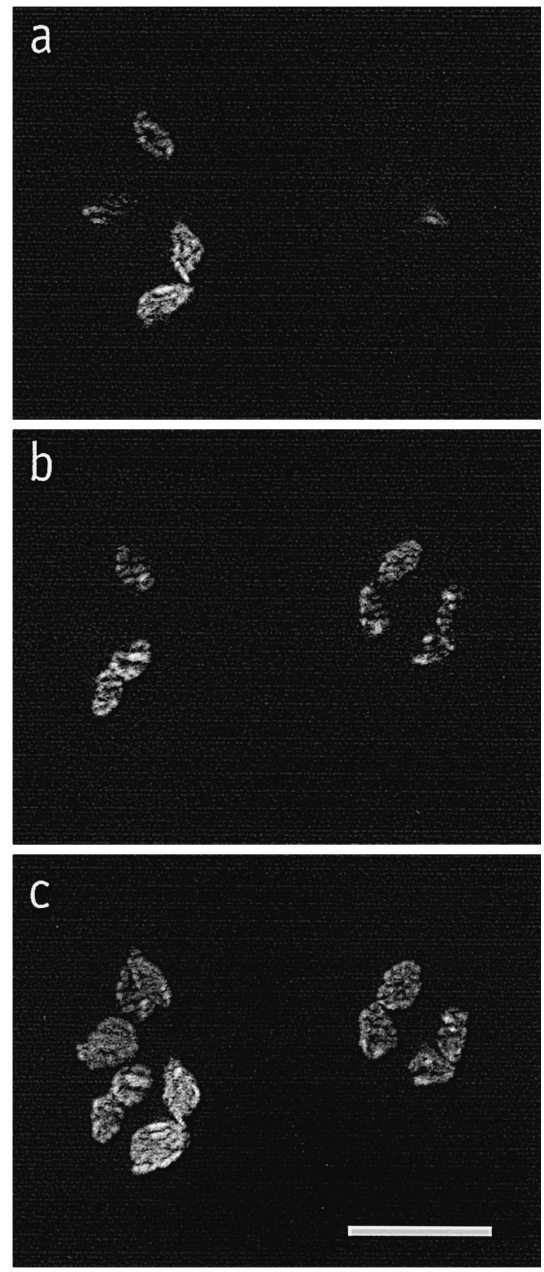

Fig. 3. Autofluorescence images of the spores of the moss *Polytrichum commune*. (a), (b) Single image slices taken at focal settings 3 μm apart. (c) Autofocus image obtained from the whole specimen volume. The scale bar represents 10 μm.

phase ϕ_0 was controlled by the piezo driven mirror in one of the beam paths. This was driven in a simple saw-tooth fashion synchronised to the camera frame rate such that any three successive camera images corresponded to the spatial shift of the fringe pattern of one third of a period. The optically sectioned images were obtained using Eq. (4) in the form of a look-up table which mapped all possible combinations of I_1, I_2 and I_3 from our 8-bit frame grabber to I_p.

The optical sectioning strength was characterised by scanning a thin fluorescent sheet axially through focus. The thin sheet was made by diluting a suspension of 30-nm latex FluoSpheres (Molecular Probes) in water and depositing it on a cover glass and allowing it to dry out completely. Our experience shows that this provides a very simple method of producing sufficiently uniform thin films suitable for characterising fluorescent axial responses. The measured response is shown in Fig. 2 where we find a half width half maximum width of 0.38 μm. In our experimental setup the period of the illuminating fringes was $\Lambda = 0.68$ μm and a fluorescence wavelength of $\lambda = 680$ nm. Under these conditions Eq. (9) predicts a HWHM width of 0.3 μm which compares well with the experimentally measured value. We note that we have taken the numerical aperture of the objective to be 1.35 rather than 1.4 since previous measurements on this lens have shown this to be a more appropriate value [7].

Finally, we show autofluorescence images obtained in real time in Fig. 3. Fig. 3a, 3b show the autofluorescence from the chlorophyll in the chloroplasts in the spores of the moss *Polytrichum commune*. The fluorescence was again excited with the Ar^+ laser (488 nm) and detected at wavelengths beyond 580 nm. The two sectioned images were taken at focal settings 3 μm apart. Fig. 3c shows an autofocus image of the whole specimen volume. This image was obtained by displaying the maximum image intensity at each pixel through a 20 μm axial scan with the 100×1.4 numerical aperture objective lens.

5. Conclusions

We have presented a very simple method to obtain real time optically sectioned fluorescence images from a wide-field conventional microscope. The method, which is based on spatial heterodyning to provide the sectioning, provides for easy system alignment and has no restrictions on the illuminating wavelength.

Acknowledgements

This work was supported by the Paul Instrument Fund of the Royal Society. We thank B. Sarafis for providing the *Polytrichum commune* specimen.

References

[1] T. Wilson, C.J.R. Sheppard, Theory and Practice of Scanning Optical Microscopy, Academic Press, London, 1984.
[2] T. Wilson (Ed.), Confocal Microscopy, Academic Press, London, 1990.
[3] J.B. Pawley (Ed.), Handbook of Biological Confocal Microscopy, Plenum, New York, 1995.
[4] M.A.A. Neil, R. Juškaitis, T. Wilson, Opt. Lett. 22 (1905) 1997.
[5] M. Born, E. Wolf, Principles of Optics, 5th edn., Pergamon Press, Oxford, 1975.
[6] P.A. Stokseth, J. Opt. Am. 59 (1969) 1314.
[7] T. Wilson, R. Juškaitis, Bioimaging 3 (1995) 35.